Engineering and Technology Journal
Journal homepage: https://etj.uotechnology.edu.iq

Parametric evaluation and biomechanical assessment of a curved biodegradable ZK60 locking plate for femoral shaft fractures using finite element analysis

Ahmad S. Jasim [a*], **Jenan S. Kashan** [b], **Aseel H. Abed** [a]

[a] College of Production Engineering and Metallurgy, University of Technology-Iraq, Alsina'a street, 10066 Baghdad, Iraq.
[b] College of Biomedical Engineering, University of Technology-Iraq, Alsina'a street, 10066 Baghdad, Iraq.
*Corresponding author Email: pme.20.66@grad.uotechnology.edu.iq

HIGHLIGHTS

- A novel curved biodegradable ZK60 locking plate was designed for femoral fracture fixation.
- Finite element analysis showed that 6 mm plates had 10% higher axial stiffness than 4 mm plates.
- Plate bending angles of 15°–20° improved load distribution and reduced stress concentrations.
- The combined effects of thickness and curvature produced optimal biomechanical implant stability.

Keywords:

Bone plate stiffness
Fracture fixation
Finite element analysis (FEA)
ZK60 Magnesium Alloy
Biodegradable implants
Femoral shaft fracture
Parametric assessment

ABSTRACT

This study evaluates the biomechanical performance of a novel curved biodegradable ZK60 magnesium alloy locking plate for plate osteosynthesis in midshaft femoral fractures classified as AO/ASIF 32-A3 (Arbeitsgemeinschaft für Osteosynthesefragen/Association for the Study of Internal Fixation). Current metallic implants are associated with complications such as stress shielding, the need for secondary surgery, and limited support for biological healing. Biodegradable options offer promising solutions but remain insufficiently studied, especially regarding curved plate designs. This work addresses that gap by systematically assessing how plate thickness and curvature influence fracture stability. Finite element analysis (FEA) was performed under physiological loading of 700 N simulating a single-leg stance. Ten configurations were modeled, combining two thicknesses (4 and 6 mm) with five bending angles (0, 5, 10, 15, and 20°). A 5 mm fracture gap was simulated, and all constructs were fixed with bicortical locking screws. Axial stiffness and total deformation were calculated and compared with those of an intact femur. Results indicated that both increased plate thickness and curvature enhanced construct performance. The 6 mm plate bent at 20° showed the highest stiffness (2328.9 N/mm) and lowest deformation (0.3007 mm), representing a 6.6% increase in stiffness and 5.8% reduction in deformation compared with the flat counterpart. Similar trends were observed for the 4 mm plate. The evaluated designs achieved 23.8–25.4% of intact femur stiffness, aligning with the biomechanical window that promotes callus formation through controlled micromotion. Curved configurations also improved load transfer and screw alignment. Among the tested designs, the 6 mm plate bent at 15°–20° demonstrates the most favorable biomechanical characteristics for potential clinical translation.

1. Introduction

Fractured lower leg, especially the mid-shaft fractures, is one of the most common injuries occurring in traumatic events involving motor vehicles [1]. Most fractures that have narrow medullary canals are usually fixed using orthopaedic plates [2]. Strength in internal fixation devices is often undermined because of some design features that fail to match the mechanical demands that occur during bone healing [3-5]. Bone healing occurs because of interfragmentary movement (IFM) that exists between 1 and 3 mm, and this motion influences both bone healing processes and mechanisms [6,7]. It is reported that the fracture fixations' stiffness stands as a primary determinant factor of interfragmentary motion [8,9] while 0.2-1 mm perpendicular micromovement helps speed up secondary healing through callus development [10]. Though the empirical studies are vast, the balance between rigid and flexible plate structures is still disputed [11].

http://doi.org/10.30684/etj.2025.162401.1983
Received 11 July 2025; Received in revised form 24 August 2025; Accepted 09 September 2025; Available online 28 October 2025
2412-0758/University of Technology-Iraq, Baghdad, Iraq

The locked plating systems have several biomechanical benefits, including their use in the treatment of osteoporotic fractures or cases of poor reduction, which explains their popularity in present-day orthopedic surgery [12,13]. Orthopaedic implantation systems designed to enhance bone repair after fracture offer two main advantages: higher biological support, which facilitates fracture healing, and improved fixation mechanics [14]. The remedies of locking plate technology include locked plating along with minimally invasive plating techniques and stable construct achievement without necessitating plate-bone interface friction [15-17]. The contrasted screw-plate structures produce a single-beam-like response in terms of the predetermined orientations of screws, with plates altering the transmission of loads compared to traditional plates [18-20]. Locking plates distribute mechanical loading mainly by compression at the bone-screw interface, in contrast with fixing in traditional constructions that distribute load mainly by friction at the plate-bone interface, thus offering better results in areas of low bone density [21,22].

Because of their beneficial degradation and biocompatibility properties, biodegradable materials, in particular alloys consisting of magnesium, have been suggested as replacements to conventional materials [23]. According to Singh et al. [24], magnesium alloy osteosynthesis plates experience a constant mechanical strength reduction, which leads to a weakness level approximately 65% below that of titanium plates. The discovery highlights important obstacles affecting the mechanical reliability of magnesium-based implants, as it is vital for their successful use in bone fixation.

Nonetheless, Zhang et al. [25], identified magnesium as an attractive material for biodegradable implant development according to their study. Magnesium alloys showed superior properties to conventional materials because they have mechanical responses similar to bone tissue, thus reducing stress shielding and potential implant removal surgeries. Also, Jayasathyakawin et al. [26], in their new article revealed the chemical degradability of the Mg-based materials as well as suggested them as a replacement for commonly used materials. A complete review of the lifecycle of magnesium-based implants was completed by Luo et al. [27], proving their clinical feasibility in the field of bone healing. A systematic review conducted by Lu et al. [28], supported the effectiveness of magnesium in comparison to titanium further and suggested high-quality clinical trials. Wang et al. [29], also provided the argument for the antibacterial properties of the Mg, Fe, and Zn alloys, along with their twofold infection prevention and mechanical assistance features. At the same time, Zhang et al. [30], discussed carbon-fiber-reinforced PEEK as an alternative with minimized effects of stress shielding but sufficient mechanical performance. Together, these experiments give credence to the developing evidence that suggests the beneficial position of biodegradable materials, especially Mg-based alloys, as potential options to replace conventional implants. The biomechanical analysis by Hu et al. [31], demonstrated that biodegradable materials serve to stimulate bone remodeling under load conditions. A combined design strategy that integrates biodegradable and traditional materials has received support from researchers based on their findings regarding initial strength and fatigue resistance properties in biodegradable implant development.

Research conducted by Al-Tamimi et al. [32], applied topology optimization techniques to bone fixation plate development. The researchers demonstrated that optimized implants utilize more effective bone loading mechanics for enhanced fracture site stability. The research confirmed that maintaining proper stiffness with reduced stress shielding effects could be achieved through the combination of sufficient plate stiffness and selective laser melting (SLM) and electron beam melting (EBM) manufacturing techniques. Al-Tamimi [33], published in 2021 to extend research about three-dimensional topology optimization of Locking Compression Plates (LCPs). The research objective was to reduce stress-shielding effects and achieve effective bone restoration function. Elastic modulus matching existed between the optimized topology designs and natural bone tissue, demonstrating important improvements in designing internal fixations.

Recent work has evaluated biodegradable materials, especially magnesium alloys, for orthopedic fixation. These studies report acceptable biocompatibility and bone-like mechanics, which may reduce stress shielding, while also highlighting open issues such as degradation rates, corrosion behavior, and long-term strength. Advances in design and manufacturing, including topology optimization and additive manufacturing, aim to tailor stiffness and geometry for fracture fixation [23-33].

Taken together, prior literature shows that implant performance depends on material properties, plate geometry, and screw configuration. Effective designs must balance construct stiffness for stability with enough flexibility to allow controlled micromotion that supports secondary healing. However, the biomechanical performance of curved biodegradable locking plates, particularly those based on magnesium alloys, has not been systematically investigated. This gap limits understanding of whether such designs can provide adequate fixation while avoiding stress shielding and promoting bone healing.

The objective of this study is to evaluate the biomechanical effects of plate thickness and curvature in a curved ZK60 locking plate for AO/OTA 32-A3 femoral shaft fractures using finite element analysis. Axial stiffness and total deformation were assessed relative to an intact femur under physiological loading. By focusing on these key design variables, the study aims to generate evidence that can inform the future development of biodegradable fixation plates.

2. Methods and materials

2.1 General strategy

Finite element analysis (FEA) was used to assess the mechanical performance of biodegradable ZK60 locking plates for mid-shaft femoral fractures. FEA enables simulation of structural behavior under specific loading and boundary conditions, reducing the need for physical prototyping [34,35]. Models replicated femoral geometry, material properties, and single-leg-stance boundary conditions. An intact femur served as the reference. Ten plate configurations combined two thicknesses (4 and 6 mm) with five bending angles (0°, 5°, 10°, 15°, 20°). All constructs used biodegradable bicortical locking screws. Outcomes were axial stiffness and total deformation. The bending conditions for both thicknesses are summarized in Table 1.

A vertical axial load of 700 N was applied at the femoral head with the distal femur fully constrained to represent a static single-leg stance. The 700 N value approximates one body weight for a 70 kg adult and is widely adopted in femoral biomechanics and FEA studies of fracture fixation [36-38].

To reflect different clinical philosophies, flat plates (0°) were considered higher-stiffness constructs for immediate post-operative stability. In contrast, bent plates (5°–20°) represented lower-stiffness constructs that promote controlled interfragmentary motion during secondary healing [7,8,10]. This framing allows for the evaluation of stiffness–flexibility trade-offs without implying optimization.

Table 1: Plate bending conditions used for both thicknesses (4 and 6 mm)

Model	Bending Angle (°)	Structural State
1	0	Flat
2	5	Bent
3	10	Bent
4	15	Bent
5	20	Bent
Intact	—	Unfractured (Control)

2.2 Computational analysis

2.2.1 Clinical models analyzed

The control model consisted of an intact femur displaying a 16 mm diameter hollow intramedullary canal as well as a total length of 470 mm. The femur specimens underwent modifications between Models 1 and 5 through the creation of a 5 mm midshaft defect, which was positioned at 235 mm above the lower end. Designed the midshaft defect to mimic the 32-A3 transverse fracture, which represents a widespread diaphyseal fracture based on the AO Foundation classification. The transverse fracture pattern of two femur segments develops at the midshaft region of the bone, showing a fracture angle lower than 30 degrees [36,39-41]. The 5 mm gap was selected to simulate a critical defect condition commonly adopted in biomechanical and computational studies [40], even though it does not represent the ideal fixation scenario for an AO/ASIF 32-A3 fracture. This approach allows for conservative testing of plate stability.

A biodegradable ZK60 magnesium alloy locking plate measured 192 mm in length with 9 holes and existed in two thicknesses of 4 mm and 6 mm. These thicknesses were selected based on a combination of biomechanical and clinical considerations: 4 mm provides standard mechanical stability for diaphyseal fractures. In comparison, 6 mm offers additional support in higher-load scenarios without exceeding typical clinical ranges, thus ensuring sufficient stability and biological healing [refer to Section 2.2.2.2]. The selection of nine holes was made following AO/OTA guidelines, which recommend a minimum of three bicortical screws per main fragment for stable fixation [41,42]. The hole configuration also adheres to the principle of maintaining an appropriate working length to avoid stress concentration, especially over the fracture site, ensuring better load distribution and promoting biological healing through micromotion control. The fixation involved using eight bicortical locking screws with 5 mm diameter and 50 mm length from the same manufacturer (AO surgical principles were used to position the screws, four in each main fragment, and the central hole remained empty to decrease stress concentration and promote biologic healing conditions). The production of plates and screws involved the same ZK60 magnesium alloy to maintain material uniformity [37]. The computational model allowed a detailed assessment of the mechanical performance of the plate-screw system for securing 32-A3 transverse fracture patients under authentic clinical scenarios. The analysis relied entirely on finite element modeling (FEM), simulating the mechanical behavior of the construct under applied loads.

2.2.2 CAD Models

2.2.2.1 CAD Model of an artificial femur

This research made use of an artificial femur CAD model obtained from Sawbones (Vashon, WA, USA) (Figure 1). Its development protocol has been validated in prior studies [36,39,43]. The radiological scans of the artificial femur were performed end-to-end at 0.5 mm spacing. The CT scans were transferred to Mimics Medical Imaging Software (The Materialise Group, Leuven, Belgium) to generate a three-dimensional model based on DICOM format. The exported 3D model moved from Mimics Medical Imaging Software (The Materialise Group, Leuven, Belgium) to the SolidWorks CAD program (SolidWorks Corp., Dassault Systèmes, Concord, MA, USA) for enhanced model development [36-40,42-44].

The CAD model properly simulated the complete structure and materials of cortical and cancellous bone components. The initial design of the model did not include an intramedullary canal until the "cut" operation in SolidWorks was performed, which added this feature. A 5 mm bone gap was incorporated at the midshaft of the femur through the "cut" SolidWorks operation in Models 1 to 5. Research data indicate that the femur model possesses geometry characteristics identical to those in previous study designs [37,42,43]. The femur received tetrahedral elements of uniform shape and dimensions for its meshing process.

SolidWorks 2024 CAD program from SolidWorks Corp. (Dassault Systèmes), based in Concord, MA, USA, generated the models for the metal plate and screws. The experimental measurements obtained with precision Vernier calipers served as the foundation for creating these models, as reported in previous research papers [37,42,43]. The SolidWorks application saved CAD data in the Parasolid file format (IGS) to enable seamless interoperation with ANSYS software analysis.

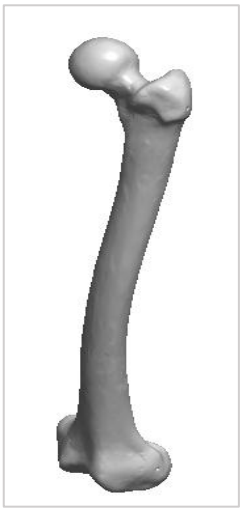

Figure 1: CAD model of an artificial femur

2.2.2.2 Geometrical model of a bone plate

The baseline geometrical dimensions of the plate (length, width, thickness, and number of holes) are detailed in Section 2.2.1. This subsection addresses only the bending modifications, comparing the flat plate (0°) with curved plates bent at 5°, 10°, 15°, and 20°, as illustrated in Model 1 (Table 1) and Figures 2a and 3a. The flat plate design undergoes bending in the center at four different angles starting from 5° up to 20° (Models 2 through 5 in sequence) as represented in Table 1and Figures 2b and 3(b-e) to establish the most suitable design configuration. The test sample comprises bent plates that are compared against an equivalent flat bone plate with similar dimensions.

The selection of the bending angle range 0°–20° was based on clinical practice and anatomical constraints. A flat plate (0°) represents the conventional starting point in bone fixation, while the bending angle is gradually increased up to 20° to simulate realistic, moderate curvature for better anatomical conformity. This range aligns with typical orthopedic practice, where moderate bending is used to improve plate fitting and load distribution across the fracture site, ensuring biological healing conditions [37] [43]. Higher bending angles (greater than 20°) were avoided, as they could introduce unnecessary rigidity, which would limit micromotion and negatively impact fracture healing [45]. FEA software accepts designed files exported from the analysis software in formats including ANSYS Workbench for further evaluation [34,45].

2.2.2.3 Traditional flat plate

The standard flat design of a bone plate has a dense, linear design and a circular contouring that are meant to maximise patient comfort as well as the efficiency of the fixation. Here are the findings displayed in Tables 1 and 2 and Figures 2a and 3a from Model 1. The CAD model of the traditional flat plate maintains a 192 mm length with a 30 mm width and two thicknesses of 4 mm and 6 mm. The plate design contains nine strategically placed holes intended specifically for screw fixation, which works as the main stability method. The plate has established screw openings that support locking cortical screws measuring about 5 mm in diameter, which represents an industry standard for long bones within the femur.

The plate provides multiple screw holes, but surgeons need not install all these holes at once. The mechanical stability of bones, especially in the femur area, becomes compromised by extended drilling activities, preventing the implementation of screw stabilization in these load-bearing areas. Multiple screw holes on the implant enable surgical choice of ideal holes for stable fixation solutions, which prevent unneeded bone destruction. The top surface of the bone plate incorporates rounded edges through a filleted design to reduce potential soft tissue injuries to patients. Traditional flat plates demonstrate limitations as femur bone support systems because they lack the required strength in severe bone fracture cases, so researchers continue to design better plate alternatives [34].

2.2.2.4 Developed design (Bent)

Flat bone plates have traditionally been manufactured in small dimensions with flat contours. The bone plate dimensions have been expanded to reach larger spans of the target bone tissue during this development. The long bone-specific design of this plate provides limited support to the bone when its edges detach from the bone surface because it was created for femur applications only. Because the flat plate installs onto a cylindrical-shaped long bone, it creates this problem.

Medical practitioners increasingly design implants specifically for individual patients in current medical practices. Bent implant development became necessary since it supports more accurate bone-shape adaptation, specifically for long bones, including the femur. The 3D CAD visual in Figure 2b shows the newly produced bent bone plate, and Figure 3 displays its defined bending angle from b to e. Bent bone plates feature central curvature, which follows bone surfaces naturally to achieve better alignment than flat plates. Researchers believe the curved shape both stabilizes bone fragments excellently while providing greater comfort to patients. The bent plate shows potential to shorten recovery times and enhance clinical outcomes for orthopedic applications, which makes it an effective choice for orthopedic applications [45].

(a) (b)

Figure 2: Showing an isometric view of a locked bone plate: a) Traditional Flat Plate, and b) bent plate

(a) (b) (c) (d) (e)

Figure 3: shows a side view of the bone plate according to the model

2.2.2.5 Locking cortical bone screw

A custom-designed locking cortical bone screw was developed from ZK60 magnesium alloy, aiming to combine biodegradability with high mechanical strength for orthopedic applications. The screw was designed in SolidWorks 2024 and features a major thread diameter of 5 mm, a core diameter of 4 mm, and a thread pitch of 1.5 mm. The threading profile follows a 30° buttress angle, optimized to maximize pull-out resistance, as illustrated in Figure 4 [26,27].

The head of the screw incorporates a 10° conical taper, reducing from 8 mm at the top to 5 mm at the base, ensuring tight locking compatibility with bone plates [26]. The screw also features a hexalobe drive specifically designed for locking plate systems. It includes a self-tapping fluted tip for easier insertion and offers an optional self-drilling version to enhance surgical handling. The complete CAD geometry covering thread configuration, head shape, and insertion design was modeled with high accuracy in SolidWorks [27,37].

In clinical scenarios, this locking screw performs well in weight-bearing applications such as femoral fracture fixation and orthopedic stabilization. Its biodegradable nature eliminates the need for secondary removal surgery and reduces stress shielding—thereby enhancing bone regeneration and long-term fixation outcomes [24,29,45].

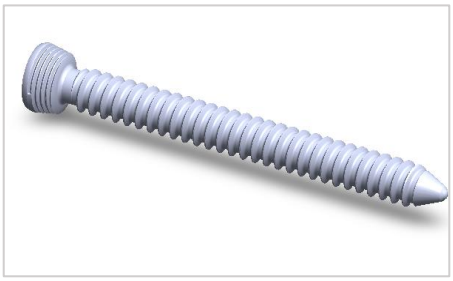

Figure 4: Locking cortical bone screw

2.2.3 Assembly of components

The SolidWorks software was used to build the femur-plate-screw construct by combining individual part models in Figure 5. This model was transferred to ANSYS Workbench R24, where FEA took place while adhering to AO surgical approaches by distributing eight bicortical screws (5mm diameter, 50mm length) symmetrically, except leaving the screw hole adjacent to the 5mm fracture gap empty for balancing mechanical strength with biological healing potential.

Contact interactions were simulated using CONTA174 surface-to-surface contact elements with three translational degrees of freedom (x, y, z) interfacing with TARGE170 targets, with identical real constants assigned to both element types and all interfaces modeled as fully bonded to represent rigid connections [43,46], creating a biomechanically optimized assembly that balanced load transfer, minimized stress concentrations, maintained fixation strength, and preserved the fracture microenvironment by AO Foundation guidelines.

2.2.4 Meshing and element quality

The analysis of the femur, plate, and screws mesh was conducted in ANSYS Workbench 2024. The femoral bone and the locking plate were modeled using SOLID186 elements for the bone and SOLID45 for the plate, which are widely applied for solid structural modeling in finite element analysis [34,35]. For the cortical bone, a tetrahedral mesh with 10-node quadratic elements was adopted, consistent with previous femoral FEA studies [36,37]. To improve accuracy, mesh refinement was applied in the fracture region to capture stress concentrations, while a coarser mesh was applied elsewhere to maintain computational efficiency [42,46].

A multi-layer strategy was applied to represent the plate and bone thickness. The cortical bone was modeled with two layers across its thickness. In contrast, the cancellous bone was simplified as a homogeneous isotropic material, a practice often adopted in large-scale femoral simulations to balance accuracy and computational cost [9,38,43]. This approach ensured that the model preserved the essential mechanical behavior of bone under load while avoiding unnecessary computational complexity.

The final mesh evaluation yielded 529,564 to 1,025,371 nodes and 358,438 to 691,563 elements, depending on model configuration [42,46]. The cortical bone region was discretized with the same 10-node quadratic tetrahedral elements used for metallic components. Quadratic triangular contact elements were applied at the bone–metal interfaces. In contrast, quadratic quadrilateral contact elements were assigned to the loading platen, ensuring accurate representation of interface behavior and load transfer [34,35]. The overall meshing strategy produced high-quality elements, enabling precise geometric representation, efficient convergence, and reliable finite element analysis results.

Mesh quality evaluation demonstrated a skewness value of 0.28017, indicating high-quality mesh elements with minimal distortion, as shown in Figure 6. A refinement of the bone model was carried out to use 2.0 mm element sizes for improved precision, especially in the region around the fracture gap. The mesh settings also incorporated a precise relevance center, high smoothing, and a gradual transition, which enhanced both simulation accuracy and robustness. These adjustments allowed for an efficient convergence of results during analysis, ensuring reliable predictions of mechanical behavior in the FEA model [34,35]. The meshing strategy, which combines high precision in critical areas with computational efficiency, guarantees both the accuracy of the geometry and the reliability of the results, as depicted in Figure 7 [42,46].

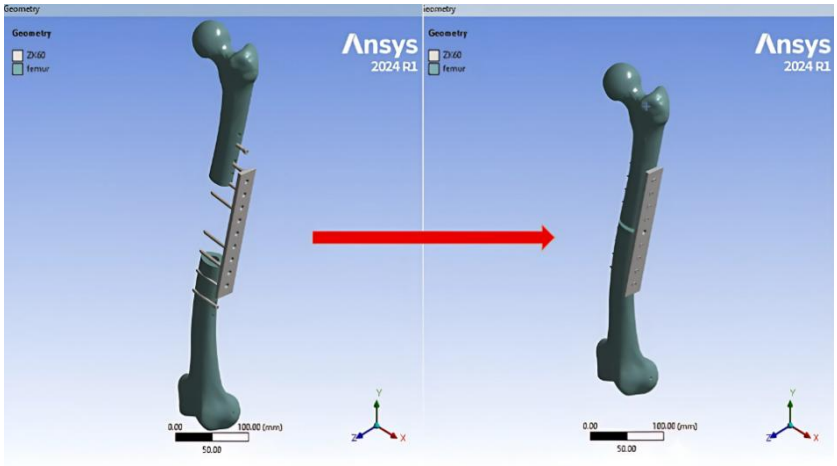

Figure 5: Assembly of the bone plate of the finite element models

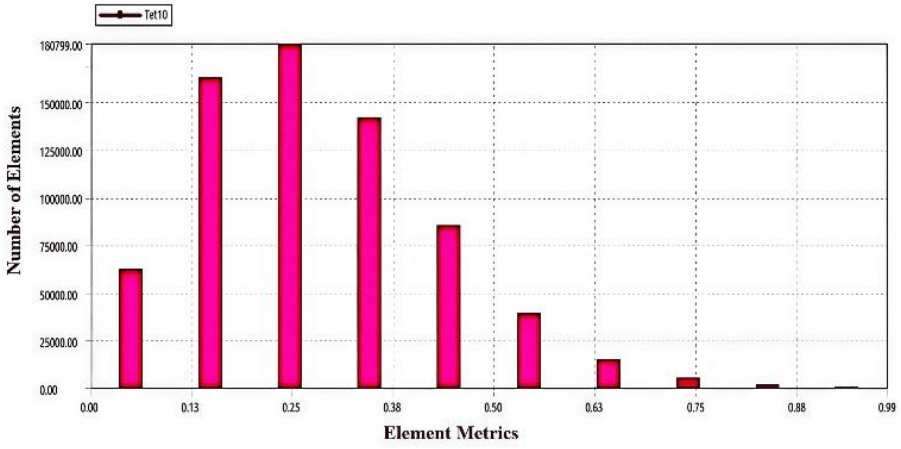

Figure 6: The average skewness values of the finite element models

2.2.5 Material assignments

Assigning material properties to human bone models presents a unique challenge due to the heterogeneous and anisotropic nature of biological tissues. However, for this finite element study, the femur was modeled as an isotropic material, assuming uniform properties in all directions. This approximation is commonly used in large-scale simulations focusing on the structural behavior of the entire femur [9,36,38,43].

Material properties were assigned through the Engineering Data module in ANSYS Workbench. The femoral cortical bone and the ZK60 magnesium alloy used for the plate and screws were defined according to validated mechanical parameters, as shown in Table 2. Specifically, the femoral cortical bone was treated as an isotropic material with an elastic modulus of 16.7

GPa and Poisson's ratio of 0.3, which is a standard approximation used in large-scale FEA for bone models. The ZK60 magnesium alloy for the plate and screws was assigned an elastic modulus of 44.8 GPa and Poisson's ratio of 0.35 [21].

This material assignment ensures an accurate stress-strain response for all components under the applied loading conditions. The modeling of the femoral bone did not include plastic material properties, as the study focused on evaluating the elastic behavior of the system under static loads. Since the maximum stresses observed in the finite element analysis were well below the yield strength of the materials (ZK60 magnesium alloy has a yield strength of approximately 220 MPa), the materials remained within their elastic limits, ensuring no plastic deformation occurred during the simulations.

The assumptions made for elastic behavior align with the static loading conditions modeled in this study, where the primary goal was to assess the mechanical stability and deformation of the locking plate under physiological loading conditions.

Table 2: Material properties

Material	Density (kg/m³)	Young modulus (GPa)	Poisson ratio
Cortical Bone [38]	1750	16.7	0.3
ZK60 magnesium alloy [21]	1830	44.8	0.35

2.2.6 FEA Boundary conditions

The boundary conditions applied in this study were based on validated protocols from previous computational models simulating femoral fracture fixation [42,43,47]. All interfaces between the plate and screws, as well as between the femur and screws, were modeled as bonded contacts to replicate stable fixation and simulate full mechanical interlocking. This simplification excluded the geometric modeling of screw threads while preserving the effect of full cortical engagement, which is consistent with osseointegration behavior observed in vivo [42].

The inclusion of screws in the finite element (FE) model, despite the bonded contact assumption, is necessary for several reasons. First, the screws are included in the model to ensure proper alignment and placement within the locking plate and femur. This ensures the correct geometry and load transfer from the plate to the bone, providing accurate predictions of the mechanical behavior of the construct [47]. Second, while the bonded contact assumption simplifies the analysis by ignoring frictional effects and screw thread interactions, the screws remain critical in simulating the fixation mechanism and load-bearing behavior of the entire system. This allows for accurate stress distribution and deformation analysis across the screws and bone-plate interfaces [43]. Third, by modeling the screws explicitly, the interaction between the screws and the cortical bone can still be captured, ensuring realistic stress analysis in the bone and surrounding tissues, even when frictional forces are neglected [42].

In clinical settings, implanted devices are often surrounded by newly formed bone, validating the use of bonded interactions in simulations [43]. To replicate real-world loading tests, the femoral head was allowed only vertical displacement (Y-axis). At the same time, horizontal movement (X and Z axes) was restricted by bonding the contact surface with the loading platen. The distal femur condyles were fully constrained, simulating the fixed support used in biomechanical experiments [47].

These boundary conditions were chosen to replicate the conditions found in experimental and clinical studies realistically. The use of vertical displacement at the femoral head simulates the physiological loading seen during a single-leg stance. The restriction of horizontal motion helps mimic the rigid fixation of the femur during in-vitro tests. The full constraint of the distal femur condyles is consistent with common biomechanical testing protocols, where the distal femur is typically fixed to ensure proper alignment and prevent any movement that might interfere with the analysis of load distribution and mechanical behavior [42]. An axial load of 700 N was applied through the loading platen surface to mimic single-leg stance conditions, which is approximately equal to the body weight of a 70 kg individual. This value falls within the range of single-leg stance loading reported in literature, thus making it an appropriate choice for simulating the mechanical conditions experienced during walking or standing [47]. Figure 8 presents the complete boundary setup, reproducing realistic mechanical constraints for the femur-implant construct.

Figure 7: Meshing of the finite element models

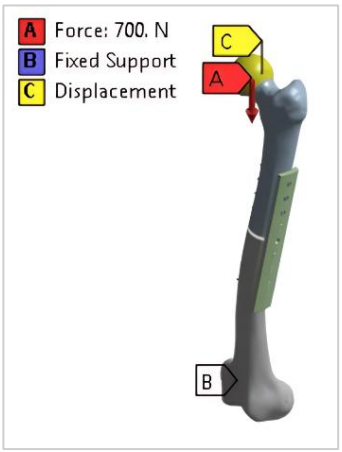

Figure 8: Boundary conditions of the finite element models

2.2.7 Finite element analysis (FEA) approach

ANSYS Workbench 2024 Suite was employed to simulate femoral constructs under a 700 N axial load. This loading condition corresponds to the single-leg stance phase of a 70 kg human body and has been clinically validated in previous studies [42,43]. Axial stiffness for each configuration (The models tested in the FEA included Models 1 through 5, along with the intact femur (control model)) was calculated using Equation (1):

$$\text{Stiffness (k)} = \frac{F}{\delta} \quad (1)$$

where: F = 700 N is the applied force; δ is the vertical displacement measured at the femoral head apex, the point of force application.

This approach ensured precise and reproducible stiffness measurements aligned with established physical laws and simulation standards. The FEA boundary conditions and loading strategy were implemented to match clinical and experimental test setups.

Figure 9 illustrates the algorithmic structure and workflow of the finite element analysis performed in this study.

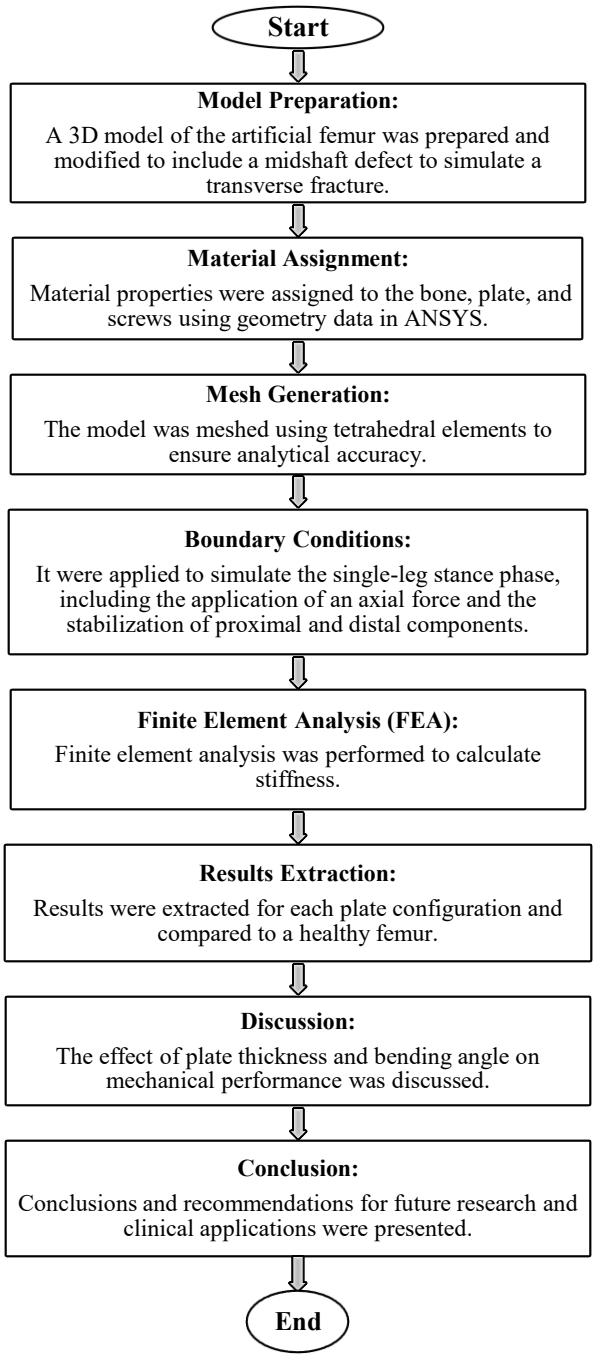

Figure 9: Research methodology steps for simulating femoral fracture fixation

3. Results

All bone plate configurations passed the Finite Element Analysis (FEA) under a 700 N axial load, simulating the single-leg stance phase according to references [37,42,43]. The analysis determined the axial stiffness and total deformation for each simulated model. Detailed findings are presented in Figures 10 through 13 for both 4 mm and 6 mm plate thicknesses. The 4 mm plates exhibited stiffness changes from 2,117.3 N/mm (Model 1 at 0°) to 2,190.4 N/mm (Model 5 at 20°), resulting in a 3.5% improvement. The total deformation decreased by 3.4%, from 0.33067 mm to 0.31958 mm. The 6 mm plates demonstrated better overall stiffness, with a maximum stiffness value of 2,328.9 N/mm (at 20°), showing a 3.2% increase, and a reduction in deformation to 0.3007 mm at this bending angle.

The control group (intact femur) displayed the highest stiffness value of 9,187.6 N/mm and the lowest deformation value of 0.076189 mm compared to all plate constructs. The stiffness values for the 6 mm plates exceeded those of the 4 mm plates by approximately 6.6% at all tested angles. The highest plate performance was observed at the 20° bending angle, which increased stiffness to 23.8% (for 4 mm) and 25.4% (for 6 mm) of the intact femur values. Stiffness values increased and deformation decreased across the bending angle range from 0° to 20° in these plate configurations. The data indicated that this performance improvement occurred for all tested plate thicknesses at the 20° bending angle.

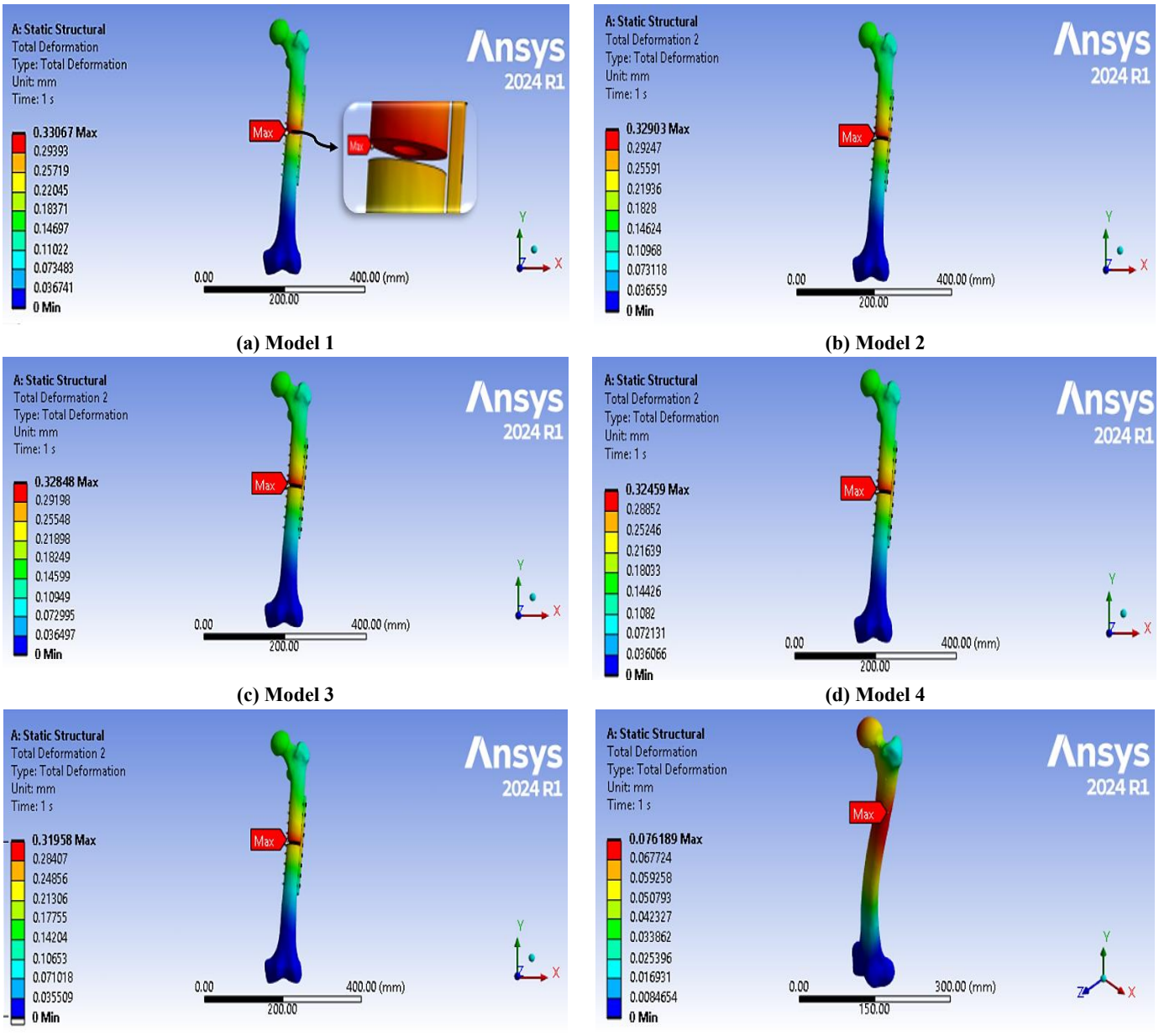

Figure 10: (a-e)Total deformation of the femur for a 4 mm thickness bone plate: Models 1 to 5 (Flat and Bent Plates) and f) Intact femur

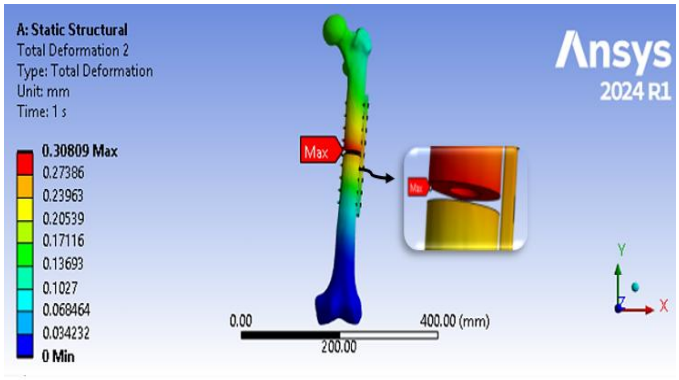

(a) Model 1

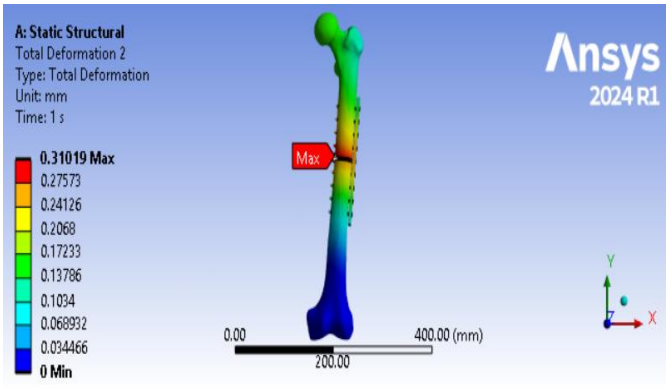

(b) Model 2

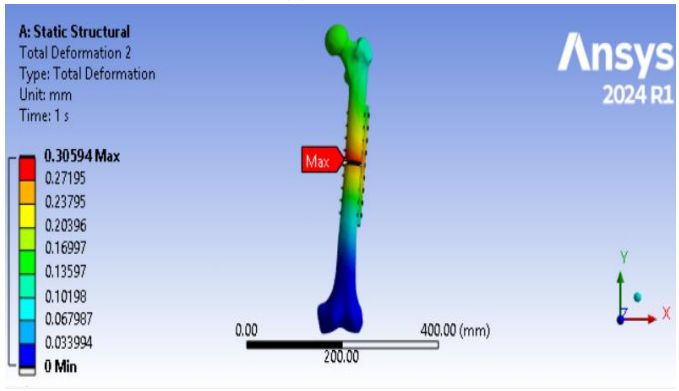

(c) Model 3

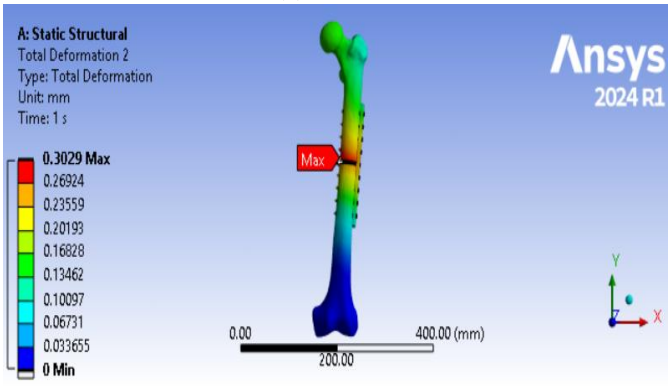

(d) Model 4

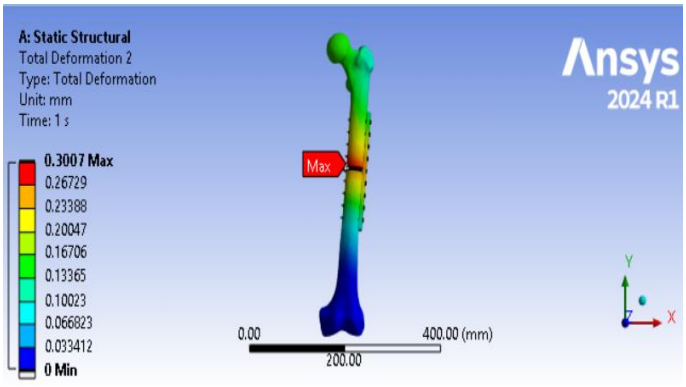

(e) Model 5

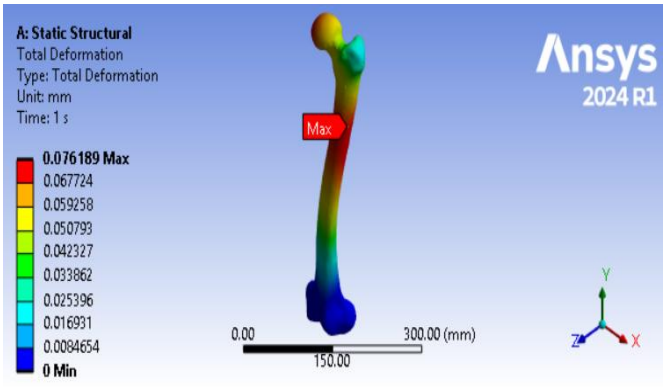

(f) Intact Femur

Figure 11: (a-e)Total deformation of the femur for a 6 mm thickness bone plate: Models 1 to 5 (Flat and Bent Plates) and f) Intact femur

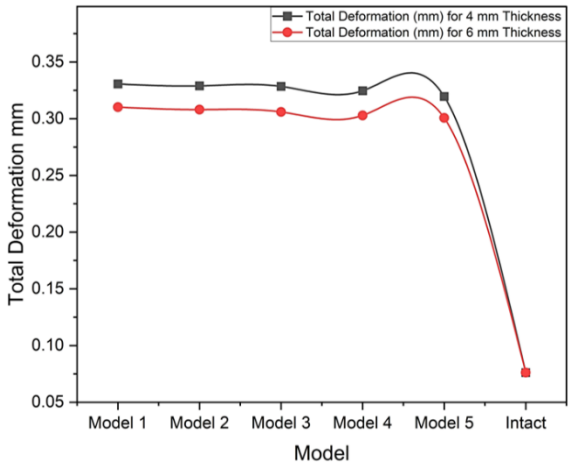

Figure 12: Comparison of total deformation mm for bone plate Models 1–5 and Intact bone with 4 mm and 6 mm thicknesses

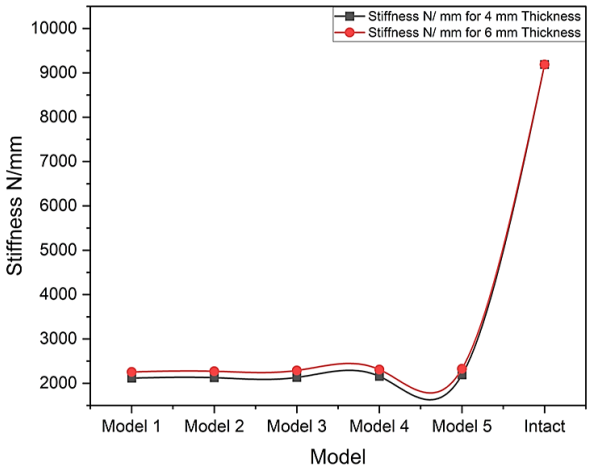

Figure 13: Comparison of axial stiffness (n/mm) for bone plate Models 1–5 and Intact bone with 4 mm and 6 mm thicknesses

4. Discussion

4.1 Effect of plate thickness on mechanical performance

The results of this study confirm that plate thickness has a decisive influence on the mechanical performance of fracture fixation constructs. The finite element simulations demonstrated that increasing thickness from 4 mm to 6 mm consistently improved axial stiffness and reduced deformation under loading. This is well explained by classical mechanics, where flexural stiffness increases with the cube of thickness ($I \propto h^3$). Consequently, even relatively small increases in thickness lead to disproportionately large increases in bending resistance [21].

For the 4 mm plates, stiffness ranged from 2117.3 N/mm in the flat configuration (Model 1, Figure 10) to 2190.4 N/mm in the 20° bent configuration (Model 5, Figure 10), with a corresponding reduction in deformation from 0.33067 mm to 0.31958 mm. Improvements were gradual as bending increased from 0° to 20°, but even at maximum bending, the stiffness achieved represented only 23.8% of the intact femur stiffness (Figure 12).

The 6 mm plates, in contrast, showed higher stiffness in all models. Starting from 2256.6 N/mm (Model 1, Figure 13) and increasing to 2328.9 N/mm in Model 5 (Figure 13), the thicker plates consistently provided superior mechanical stability. Deformation values dropped from 0.31019 mm to 0.3007 mm, and the optimal 20° bent design reached 25.4% of intact femur stiffness (Figure 13). Importantly, even the flat 6 mm plate outperformed all 4 mm plates, highlighting thickness as a dominant factor in construct behavior.

Clinically, these findings suggest that thicker plates may offer advantages in patients with higher body weight or in cases where cortical bone loss reduces natural stability. The larger cross-sectional area of 6 mm plates allows for better stress distribution across the screw-bone interface, thereby minimizing the risk of screw loosening or implant failure [30]. However, this mechanical superiority must be balanced against potential long-term risks such as stress shielding. Excessively stiff implants may reduce the physiological load transfer to bone, suppress micromotion, and eventually contribute to bone resorption and delayed remodeling. Our study indicates that 6 mm plates maintain stiffness levels that remain within a range conducive to secondary healing, but further clinical studies are needed to determine whether prolonged use could predispose patients to bone loss. This highlights the importance of considering both immediate mechanical stability and long-term biological compatibility when selecting implant thickness.

4.2 Influence of bending angle on biomechanical performance

The bending angle of plates also had a measurable influence on mechanical performance, independent of thickness. Across both plate groups, increasing curvature from 0° to 20° led to an average increase in stiffness of 3.2–3.5% and a reduction in deformation of 3.1–3.4%. While the absolute values were smaller than those caused by thickness, the trend was consistent, confirming that bending angle should not be overlooked in implant design.

Geometric and mechanical effects can explain the improvement. In non-contact locking systems, stability arises primarily from the screw-plate interface rather than direct plate-bone contact. Bending alters screw trajectories, improving their angular relationship with the bone cortex, and distributing loads more evenly across the construct. This reduces eccentric loading on individual screws and enhances axial fixation. Mechanically, the curved shape also behaves more like an arch than a flat beam, providing greater efficiency in resisting axial loads [12].

In addition, residual stresses induced during cold bending create a pre-stressed state in the plate, which increases its resistance to deformation under functional loads. This explains the consistent improvements observed as bending increased from 0° to 20°. However, bending angles beyond 20° should be avoided, as excessive deformation during bending may cause microcracks or localized material damage, predisposing the plate to early fatigue failure [45,48].

The biological significance of bending is equally important. By aligning the plate more closely with the femoral axis, optimal bending improves the physiological distribution of forces across the fracture site. This creates an environment that not only enhances mechanical performance but also promotes callus formation and fracture healing by maintaining controlled micromotion.

4.3 Comparative performance relative to natural bone

Compared to intact femur stiffness, all plate configurations reduced stiffness to approximately 23.8–25.4% of the natural value. This intentional reduction is a design strategy, not a limitation. Excessive stiffness would eliminate beneficial micromotion, leading to stress shielding and delayed union [7, 24, 36]. Controlled stiffness, on the other hand, allows interfragmentary movements between 0.2 and 1 mm, a range known to stimulate callus formation and support secondary bone healing.

The bending modifications further contributed by enhancing load distribution. Instead of concentrating forces at specific screws or fracture edges, the curved plates allowed forces to be more evenly shared across the fracture zone [12]. This combination of reduced stiffness and improved force distribution mirrors the natural biomechanics of bone, creating a favorable environment for healing.

The findings demonstrate that both thickness and bending angle are critical variables that influence fixation performance. Thicker plates provide robust mechanical support, while appropriate bending optimizes load sharing and biological healing conditions.

5. Conclusion

This study addressed an important gap in orthopedic implant development by designing and testing a curved biodegradable ZK60 magnesium locking plate for midshaft femoral fracture (AO/ASIF 32-A3). Current conventional implants often suffer from a mismatch between mechanical rigidity and biological flexibility, resulting in either insufficient fixation or stress shielding. The proposed solution combines biodegradable magnesium alloy with anatomically curved plates, evaluated under finite element simulations with physiological loading conditions.

Key conclusions are as follows:

1) Plate thickness was a major determinant of mechanical behavior. The 6 mm plates consistently outperformed the 4 mm plates in axial stiffness and total deformation. The most efficient performance was observed in the 20° bent 6 mm configuration, which achieved 2328.9 N/mm stiffness and 0.3007 mm deformation. This configuration demonstrated clear superiority over thinner plates and flat designs.
2) Plate curvature enhanced screw placement and load transfer. Even without direct plate-to-bone contact, bending angles improved alignment between screws and cortical bone, allowing more effective load sharing. At 20° bending, load transfer improved while maintaining interfragmentary motion within the ideal healing range. It should be noted that the micromotion range of 0.2–1 mm was not directly measured in the simulations but rather adopted from the literature as a biomechanical target for fracture healing. In this study, micromotion was indirectly estimated by calculating total deformation at the fracture gap under a 700 N axial load. This approach provides an approximation consistent with the literature-reported range known to stimulate callus formation during secondary bone healing.
3) ZK60 magnesium alloy provides favorable mechanical and biological compatibility. Its elastic modulus is closer to bone than traditional metals, which reduces the mismatch in load transmission. The biodegradability of ZK60 enables gradual load transfer to the healing bone. The conclusion regarding decreased stress shielding is theoretical and based on biomechanical principles reported in the literature. While stress shielding was not directly measured in this study, the improved load sharing and controlled deformation observed in the simulations suggest a reduced likelihood of stress shielding compared to stiffer traditional implants.
4) The optimized configuration (6 mm thickness, 20° bending) achieved 25.4% of intact femur stiffness. This balance provides enough stiffness to support early mobilization while avoiding excessive rigidity that would suppress micromotion. The bent geometry also provided better anatomical conformity, further improving construct stability.
5) Finite element analysis proved effective for design optimization. By using validated mesh, material definitions, and boundary conditions, the modeling approach reliably identified optimal design parameters before clinical application. This supports the use of computational simulations as a predictive tool in orthopedic implant development.

In summary, the 6 mm ZK60 magnesium plate bent at 15–20° represents a biomechanically advantageous and clinically promising option for femoral midshaft fracture fixation. It combines structural performance, anatomical conformity, and biodegradability in a single construct.

Author contributions

Conceptualization, **A. Jasim**, **A. Abed**, and **J. Kashan**; data curation, **A. Jasim**; formal analysis, **A. Jasim**; investigation, **A. Jasim**; methodology, **A. Jasim**; project administration, **A. Abed**; resources, **J. Kashan**; software, **A. Jasim**; supervision, **A. Abed** and **J. Kashan**; validation, **A. Jasim**, **A. Abed**, and **J. Kashan**; visualization, **A. Jasim**; writing—original draft preparation, **A. Jasim**; writing—review and editing, **A. Abed** and **J. Kashan**. All authors have read and agreed to the published version of the manuscript.

Funding

This research received no specific grant from any funding agency in the public, commercial, or not-for-profit sectors.

Data availability statement

The data that support the findings of this study are available on request from the corresponding author.

Conflicts of interest

The authors declare that there is no conflict of interest.

References

[1] O. O. Osinaike, A. O. Adekoya, M. A. Jaiyesimi, R. A. Akinola, B. O. Balogun, Radiographic spectrums of adults with traumatic femoral shaft fracture in the South-West, Nigeria, Rwanda J. Med. Health Sci., 7 (2024) 120–130. https://doi.org/10.4314/rjmhs.v7i2.2

[2] S. N. Bhat, A. Kumar, General Principles of Orthopaedic Plating and Overview, in Handbook of Orthopaedic Trauma Implantology, 2022. https://doi.org/10.1007/978-981-19-7540-0_12

[3] G. S. Lewis, D. Mischler, H. Wee, J. S. Reid, P. Varga, Finite element analysis of fracture fixation, Curr. Osteoporos. Rep., 19 (2021) 403–416. https://doi.org/10.1007/s11914-021-00690-y

[4] P. Augat, M. Hollensteiner, C. von Rüden, The role of mechanical stimulation in the enhancement of bone healing, Injury, 52 (2021) S78–S83. https://doi.org/10.1016/j.injury.2020.10.009

[5] J. Barcik, D. R. Epari, Can optimizing the mechanical environment deliver a clinically significant reduction in fracture healing time?, Biomedicines, 9 (2021) 691. https://doi.org/10.3390/biomedicines9060691

[6] G. R. Rechter, R. T. Anthony, J. Rennard, J. F. Kellam, S. J. Warner, The impact of early axial interfragmentary motion on the fracture healing environment: A scoping review, Injury, 55 (2024) 12111917. https://doi.org/10.1016/j.injury.2024.111917

[7] Claes, L. E. 2022. Basic biomechanical factors affecting fracture healing, in Mechanobiology of Fracture Healing: From Basic Science to Clinical Application, Cham, Switzerland: Springer International Publishing, pp. 35–64. https://doi.org/10.1007/978-3-030-94082-9_4

[8] Y. Mori, M. Kamimura, K. Ito, M. Koguchi, H. Tanaka, H. Kurishima, T. Aizawa, A review of the impacts of implant stiffness on fracture healing, Appl. Sci., 14 (2024) 2259. https://doi.org/10.3390/app14062259

[9] R. I. Abed, S. J. Abbas, W. A. A. H. Alsaadan, Mechanical analysis of bone-plate construct regarding strength and stiffness, Nahrain J. Eng. Sci., 23 (2020) 89–93. https://doi.org/10.29194/NJES.23010089

[10] M. Moazen, A. Leonidou, J. Pagkalos, A. Marghoub, M. J. Fagan, E. Tsiridis, Application of far cortical locking technology in periprosthetic femoral fracture fixation: A biomechanical study, J. Arthroplasty, 31 (2016) 1849–1856. https://doi.org/10.1016/j.arth.2016.02.013

[11] Y. Gao , B. Zhang, Probing the mechanically stable solid electrolyte interphase and the implications in design strategies, Adv. Mater., 35 (2023) 2205421. https://doi.org/10.1002/adma.202205421

[12] D. R. Epari, R. Gurung, L. Hofmann-Fliri, R. Schwyn, M. Schuetz, M. Windolf, Biphasic plating improves the mechanical performance of locked plating for distal femur fractures, J. Biomech., 115 (2021) 110192. https://doi.org/10.1016/j.jbiomech.2020.110192

[13] H. Zhang, Y. Hu, X. Chen, S. Wang, L. Cao, S. Dong, J. Su, Expert consensus on the bone repair strategy for osteoporotic fractures in China, Front. Endocrinol., 13 (2022) 989648. https://doi.org/10.3389/fendo.2022.989648

[14] C. Huxman, G. Lewis, A. Armstrong, G. Updegrove, Z. Koroneos, J. Butler, Mechanically compliant locking plates for diaphyseal fracture fixation: A biomechanical study, J. Orthop. Res., 43 (2025) 217–227. https://doi.org/10.1002/jor.25968

[15] Gupta, S. 2023. Bone healing in the presence of orthopaedic implants, in Handbook of Orthopaedic Trauma Implantology, A. Banerjee, P. Biberthaler, and S. Shanmugasundaram, Eds., Singapore: Springer, pp. 1–36. https://doi.org/10.1007/978-981-15-6278-5_50-2

[16] Scolaro, J. A., Mehta, S. 2024. Tibial shaft fracture infection, nonunion, and malunion, in Prevention and Management of Common Fracture Complications, CRC Press, pp. 265–277. https://doi.org/10.1201/9781003525875-34

[17] Proctor, A. The biomechanics of locking plates used in a supercutaneous fashion. M.Sc. Thesis, The University of Guelph, Guelph, Ontario, Canada, 2024. https://hdl.handle.net/10214/28620

[18] P. Schwarzenberg, T. Colding-Rasmussen, D. J. Hutchinson, D. Mischler, P. Horstmann, M. M. Petersen, P. Varga, Biomechanical performance of a novel light-curable bone fixation technique, Sci. Rep., 13 (2023) 9339. https://doi.org/10.1038/s41598-023-35706-3

[19] Fracka, A. B. Compaction effect on different densities of cancellous bone and immediate stability of an angle-stable interlocking nail in a distal femoral osteotomy model. M.Sc. Thesis, Michigan State University, 2025. https://www.proquest.com/openview/7cf1b32d95c188ff3e8f06a6bcce7553/1?pq-origsite=gscholar&cbl=18750&diss=y

[20] S. Zhang, D. Patel, M. Brady, S. Gambill, K. Theivendran, S. Deshmukh, L. J. Leslie, Experimental testing of fracture fixation plates: A review, Proc. Inst. Mech. Eng. H, 236 (2022) 1253–1272. https://doi.org/10.1177/09544119221108540

[21] R. Zdero, K. Gide, P. Brzozowski, E. H. Schemitsch, Z. S. Bagheri, Biomechanical design optimization of distal femur locked plates: A review, Proc. Inst. Mech. Eng. H, 237 (2023) 791–805. https://doi.org/10.1177/09544119231181487

[22] Y. Deng, H. Ouyang, P. Xie, Y. Wang, Y. Yang, W. Tan, W. Huang, Biomechanical assessment of screw safety between far cortical locking and locked plating constructs, Comput. Methods Biomech. Biomed. Eng., 24 (2021) 663–672. https://doi.org/10.1080/10255842.2020.1844882

[23] N. Tipan, A. Pandey, P. Mishra, Selection and preparation strategies of Mg-alloys and other biodegradable materials for orthopaedic applications: A review, Mater. Today Commun., 31 (2022) 103658. https://doi.org/10.1016/j.mtcomm.2022.103658

[24] J. Singh, A.W. Hashmi, S. Ahmad, Y. Tian, Critical review on biodegradable and biocompatible magnesium alloys: Progress and prospects in bio-implant applications, Inorg. Chem. Commun., 169 (2024) 113111. https://doi.org/10.1016/j.inoche.2024.113111

[25] T. Zhang, W. Wang, J. Liu, L. Wang, Y. Tang, K. Wang, A review on magnesium alloys for biomedical applications, Front. Bioeng. Biotechnol., 10 (2022) 953344. https://doi.org/10.3389/fbioe.2022.953344

[26] S. Jayasathyakawin, M. Ravichandran, S. O. Ismail, Effects of hydroxyapatite addition on the microstructure and mechanical properties of sintered magnesium matrix composites, Mater. Today Commun., 35 (2023) 105582. https://doi.org/10.1016/j.mtcomm.2023.105582

[27] Y. Luo, J. Wang, M. T. Y. Ong, P. S. Yung, J. Wang, L. Qin, Update on the research and development of magnesium-based biodegradable implants and their clinical translation in orthopaedics, Biomater. Transl., 2 (2021) 188–196. https://doi.org/10.12336/biomatertransl.2021.03.003

[28] X. Y. Lu, H. X. Cai, Y. R. Li, X. Zheng, J. Yun, A systematic review and network meta-analysis of biomedical Mg alloy and surface coatings in orthopedic application, Bioinorg. Chem. Appl., 2022 (2022)1–32. https://doi.org/10.1155/2022/4529520

[29] N. Wang, Y. Ma, H. Shi, Y. Song, S. Guo, S. Yang, Mg-, Zn-, and Fe-based alloys with antibacterial properties as orthopedic implant materials, Front. Bioeng. Biotechnol., 10 (2022) 1–32. https://doi.org/10.3389/fbioe.2022.888084

[30] C. Zhang, P. Wen, Y. Xu, Z. Fu, G. Ren, Exploring advanced functionalities of carbon fiber-graded PEEK composites as bone fixation plates using finite element analysis, Materials, 17 (2024) 414. https://doi.org/10.3390/ma17020414

[31] M. Hu, M. Li, R. Ma, X. Li, X. Ren, L. Du, C. Zeng, J. Li, W. Zhang, Biomechanical analysis of titanium-alloy and biodegradable implants in dual plate osteosynthesis for AO/ASIF type 33-C2 fractures, Heliyon, 10 (2024) e26213. https://doi.org/10.1016/j.heliyon.2024.e26213

[32] A. A. Al-Tamimi, C. Quental, J. Folgado, C. Peach, P. Bartolo, Stress analysis in a bone fracture fixed with topology-optimised plates, Biomech. Model. Mechanobiol., 19 (2020) 693–699. https://doi.org/10.1007/s10237-019-01240-3

[33] A. A. Al-Tamimi, 3D topology optimization and mesh dependency for redesigning locking compression plates aiming to reduce stress shielding, Int. J. Bioprint., 7 (2021) 339. https://doi.org/10.18063/ijb.v7i3.339

[34] J. Kurniawan, S. Y. Lin, W. T. Wang, Development and finite element analysis of a novel bent bone plate, Appl. Sci., 12 (2022) 10900. https://doi.org/10.3390/app122110900

[35] K. T. S. Tsumanuma, R. A. Caldas, I. D. Silva, M. E. Miranda, W. C. Brandt, R. P. Vitti, Finite element analysis of stress in anterior prosthetic rehabilitation with zirconia implants with and without cantilever, Eur. J. Dent., 15 (2021) 669–674. https://doi.org/10.1055/s-0041-1727544

[36] J. Hu, Y. Peng, J. Li, M. Li, Y. Xiong, J. Xiao, P. Tang, Spatial bridge locking fixator versus traditional locking plates in treating AO/OTA 32-A3.2 fracture: finite element analysis and biomechanical evaluation, Orthop. Surg., 14 (2022) 1638–1648. https://doi.org/10.1111/os.13308

[37] Ü. Saraç, S. Karadeniz, A. Özer, "Ideal plate–screw configuration in femoral shaft fractures: 3D finite element analysis, J. Surg. Med., 5 (2021) 540–543. https://doi.org/10.28982/josam.925624

[38] P. K. Satapathy, B. Sahoo, L. N. Panda, S. Das, Finite element analysis of functionally graded bone plate at femur bone fracture site, in IOP Conf. Ser.: Mater. Sci. Eng., 330, 2018, 012027. https://doi.org/10.1088/1757-899X/330/1/012027

[39] F. Layher, G. Matziolis, L. N. Kayhan, M. Bungartz, O. Brinkmann, Minimally invasive internal fixation of femoral shaft fractures, a biomechanical study with a disruptive technique, Life, 11 (2021) 1254. https://doi.org/10.3390/life11111254

[40] A. Hossain, J. L. Tipper, D. Wei, A novel fracture fixation bone plate to reduce the stress-shielding effects in long bones, The Australian Biomedical Engineering Conference (ABEC), 2019, 1–4. http://dx.doi.org/10.3316/informit.979429205566950

[41] Buckley, R. E., Moran, C. G., Apivatthakakul, T. AO Principles of Fracture Management; 3rd Edition., Germany: Georg Thieme Verlag, 2018. https://doi.org/10.1055/b-0038-160824

[42] T. Wisanuyotin, P. Paholpak, W. Sirichativapee, W. Sirichativapee, W. Kosuwon, Effect of bone cement augmentation with different configurations of the dual locking plate for femoral allograft fixation: Finite element analysis and biomechanical study, J. Orthop. Surg. Res., 18 (2023) 405. https://doi.org/10.1186/s13018-023-03894-3

[43] J. Coquim, J. Clemenzi, M. Salahi, A. Sherif, P. Tavakkoli Avval, S. Shah, R. Zdero, Biomechanical analysis using FEA and experiments of metal plate and bone strut repair of a femur midshaft segmental defect, Biomed. Res. Int., 2018 (2018) 4650308. https://doi.org/10.1155/2018/4650308

[44] A. Soni, B. Singh, Design and analysis of customized fixation plate for femoral shaft, Indian J. Orthop., 54 (2020) 148–155. https://doi.org/10.1007/s43465-019-00025-1

[45] J. Kurniawan, S. Y. Lin, W. T. Wang, Development and Finite Element Analysis of a Novel Bent Bone Plate, Appl. Sci., 12 (2022) 10900. https://doi.org/10.3390/app122110900

[46] N. Fouda, R. Mostafa, A. Saker, Numerical study of stress-shielding reduction at fractured bone using metallic and composite bone-plate models, Ain Shams Eng. J., 10 (2019) 481–488. https://doi.org/10.1016/j.asej.2018.12.005

[47] J. Nourisa, A. Baseri, L. N. Sudak, G. Rouhi, The effects of bone screw configurations on the interfragmentary movement in a long bone fixed by a limited-contact locking compression plate, J. Biomed. Sci. Eng., 8 (2015) 590–600. https://doi.org/10.4236/jbise.2015.89055

[48] A. R. Mohammed, W. K. Jawad, Octagonal shape design through the use of FEA and experimental methods are created in deep drawing, AIP Conf. Proc., 3002, 2024, 060016. https://doi.org/10.1063/5.0205958